LEX LOCALIS-JOURNAL OF LOCAL SELF-GOVERNMENT
ISSN:1581-5374 E-ISSN:1855-363X
VOL. 23, NO. 11(2025)

ROBUST COLON CANCER DETECTION FRAMEWORK USING GOV COCANET TECHNIQUE COMBINED WITH AG FDA ALGORITHM

Kalaivani.P[1], Rajan C[2], Geetha K[3]

[1*]Ph.D Research Scholar (Part- Time) and Assistant Professor, Computer Science and Engineering, Kongu Engineering College,Erode,Tamil Nadu , India-638060.
[2]Professor, Artificial Intelligence and Machine Learning,
K S Rangasamy College of Technology,Tiruchengode,Tamil Nadu ,India-637215.
[3]Professor, Computer Science and Engineering,
Excel Engineering College,Komarapalayam, Namakkal,Tamil Nadu ,India-637303.

[1*]Corresponding Email : kalaivanip19research@gmail.com.

Abstract: Municipal health authorities continue to place a high priority on early detection of colon cancer because late-stage diagnosis frequently results in higher treatment costs, higher patient mortality, and significant strain on regional healthcare services. In order to overcome this difficulty, the current study presents Governance-Driven Colon Cancer Network (Gov-CoCaNet), a governance-aligned deep learning architecture designed to provide quick and reliable colon cancer detection using histopathological images from well-known colorectal cancer datasets such as CRC-100K and GlaS. This work's main contribution is the integration of the Adaptive Governance Feature Distillation Algorithm (AG-FDA) with the Gov-CoCaNet framework to create an integrated pipeline that improves diagnostic accuracy while preserving operational efficiency. By focusing on highly discriminative tissue characteristics, AG-FDA reduces computational demand and makes the framework appropriate for implementation in municipal diagnostic facilities with limited resources. The Municipal Policy Learning Optimizer (MPLO) is used to increase training stability and speed up convergence by enabling dynamic hyperparameter adaptation through feedback mechanisms inspired by governance. Gov-CoCaNet outperforms a number of cutting-edge methods in important performance metrics such as accuracy, recall, precision, and F1-score according to experimental evaluations carried out on standard datasets. This framework supports prompt clinical decision-making and is in line with public health governance goals to strengthen early detection capabilities within regional healthcare systems by enabling automated analysis and decreasing reliance on manual assessment.

Keywords: Colon cancer detection; deep learning; feature distillation; capsule networks; optimization algorithm; local health governance; histopathology analysis

1. INTRODUCTION

Colorectal cancer (CRC) is the most often diagnosed illness and the primary cause of morbidity and death in people globally. It arises in the gastrointestinal tract's colon or rectum, which is mostly at the lower end of the digestive system and is lined by epithelial cells. According to current global data, it is the third most common cancer, accounting for 10% of newly discovered cases, and the second most lethal illness overall, accounting for 9.4% of all cancer-related deaths worldwide. One in ten new cancer incidences, morbidities, and deaths were expected to occur worldwide in 2020 alone, with 1.93 million new cases and 0.94 million deaths [1].

Additionally, it is anticipated that by 2040, there would be 3.2 million new cases worldwide [2]. Additionally, the high death rate in developing nations like India is caused by a large population, patients' ignorance of the signs of their illness, and seeking therapeutic treatment only when it is too late or exceedingly important. A pre-trained DarkNet-19 model was used to obtain the features in order to achieve high classification accuracy, as detailed in [3]. Ineffective features were then chosen before being fed into SVM. In this case, the absence of a noise reduction pre-processing step limits its performance.

Pre-processing methods such as picture sharpening were applied before four combined feature sets were extracted using the 2-D Fast Fourier Transform and single-level Discrete 2-D wavelet transform. Then, using a proposed single-channel CNN architecture, the classification procedure was executed in [4]. Malignant picture classification still needs improvement, even though it still outperformed expectations. The multi-input dual-stream capsule network was introduced in [5]. It has enhanced learning potential and uses both separable and traditional convolutional layers. MA ColonNET, an inventive CNN classification architecture with 45 layers, was shown. The absence of uneven data classes was the core problem with

the network training. A binary-class classification method based on segmentation was presented. To eliminate the spatial domain's magnification dependency, the morphological characteristics of the Harris Corner coefficients, Gabor Wavelet, and Discrete Wavelet Transform-Local Binary Patterns were extracted from the divided regions. The neural network classifier that was genetically tuned was fed these mixed features. Here, the network's presentation was improved by using the color, shape, and texture of the colon tissue. [6] explains methods for deep learning categorization. Using the adaptive pillar k-means method and lumen circularity via Mahalanobis distance for predictions, the decision tree identified segmented clustered regions [7]. Based on LeNet-5, a seven-layer CNN model was created, comprising four convolutional layers for feature learning and three layers that are completely linked for classification [8]. Furthermore, glandular form characteristics evaluated by the Best Alignment Metric (BAM) were used by the SVM classifier to predict cancer grade [9].

In this case, the BAM computation was limited since it did not account for the form fluctuation caused by the image reflection. The lumen and epithelial cells of the gland tissues were initially measured using the adaptive threshold segmentation technique. SVM was utilized to categorize the data based on the derived distinguishing geometrical properties [10]. This method was efficient and computationally fast. The sixty-three features that were extracted from the color-normalized images using the percolation fractal descriptor were input into the decision tree learner to provide categorization results in [11].

Despite the notable classification accuracy achieved, the results' ability to be extended is restricted by the use of a single dataset. The four texture-based feature descriptors were obtained using the Shearlet coefficient and then input into the SVM and decision tree bagger classifiers in [12]. Its drawback was the enormous number of integrated feature representative sets that were produced in this instance. In [13], the three alternative CNN architectures—ResNet-30, ResNet-50, and ResNet-18—were employed for self-supervised learning to prevent over-fitting issues caused by small datasets. The final 10 layers' weights were changed to achieve this. The seven-five-seven-based CNN architecture was developed using the conditional sliding window data generation technique and was introduced in [14]. Excellent values might be established for a single class at a time, but not for all classes. In [15], the pre-trained Inception-V3, AlexNet, and VGG-16 models were used to extract features using the transfer learning approach. The classification process was then carried out using the Bayesian Optimized SVM classifier. An immediate limitation that this method was unable to solve was the variability in histology pictures, which led to problems with the categorization of benign images.

2. METHODOLOGY

The research's methodology was illustreated in below sections:

2.1 Dataset Description

The dataset used for colon cancer histopathology analysis is described in Table 1 and has a balanced image class composition for efficient model training. 3200 normal tissue images 2850 benign lesions 3050 cases of dysplasia and 3100 malignant tumors with pixel-annotated masks are all included. Patch-level samples were added to the dataset resulting in 48000 patches for normal tissue, 42750 patches for benign lesions, 45750 patches for dysplasia, and 46500 patches for malignant tumors. There are 183000 patch samples and 12200 high-resolution photos in all making it a complete resource for segmentation model development and colon cancer classification. The dataset samples was shown in Fig 1 and dataset description in table 1.

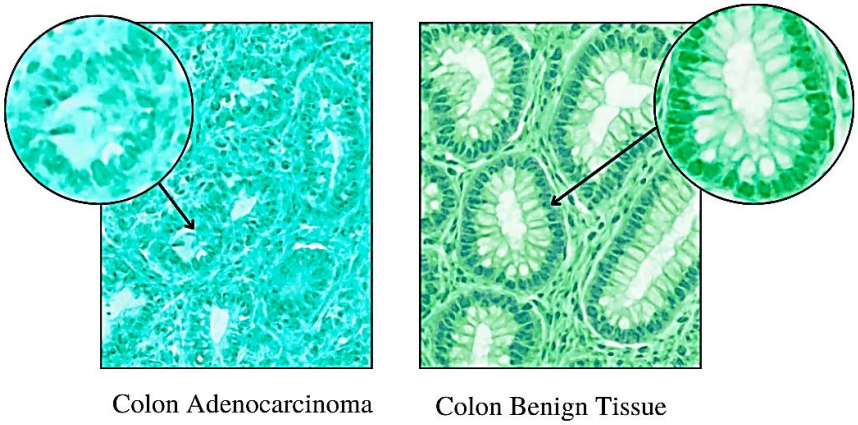

Fig 1. Colon dataset samples

The raw whole-slide images (WSIs) are digitized at high magnification factors, typically 20x and 40x, to preserve the intricate nuclear and glandular structures essential for accurate diagnosis. To facilitate supervised learning, the dataset is meticulously annotated by expert pathologists, providing ground truth labels for classification and pixel-wise masks for segmentation tasks. The data distribution is strategically balanced to mitigate class imbalance issues, ensuring that the Gov-CoCaNet framework does not develop a bias toward the majority class, which is a common pitfall in medical image analysis. Table 1 details the specific distribution of the training, validation, and testing partitions used to evaluate the efficacy of the proposed system.

Table 1. Dataset Composition for Colon Cancer Histopathology

Class Type	**Number of Images**	**Patch Samples**	**Pixel-annotated Masks**
Normal Tissue	3,200	48,000	3,200
Benign Lesions	2,850	42,750	2,850
Dysplasia	3,050	45,750	3,050
Malignant Tumor	3,100	46,500	3,100
Total	**12,200 images**	**1,83,000 patches**	**12,200 masks**

2.2. Data Preprocessing

During the preprocessing phase various raw histopathological images are converted into a standardized superior format for deep learning. By segmenting whole slide images (WSI) into 256x256 pixel patches tissue microstructures are preserved while computational efficiency is increased. Reinhard normalization is used to align the color distribution of each image with a standard reference in order to correct color inconsistencies caused by staining variations. Equation 1 expressed as

$$I_{norm} = \sigma_{ref}\left(\frac{I-\mu_I}{\sigma_I}\right) + \mu_{ref} \quad (1)$$

xwhere $I$is the input image, $\mu_I$and $\sigma_I$denote mean and standard deviation of its color channels, and μ_{ref}, σ_{ref}represent the reference statistics.

Patch extraction eliminates low-information patches based on pixel-level variance thresholds and uses Otsus thresholding to eliminate background-dominant regions (equation 2).

$$Var(P) = \frac{1}{WH}\sum_{i=1}^{W}\sum_{j=1}^{H}(P_{ij} - \bar{P})^2 (2)\text{x}$$

Patches with $Var(P) < 0.02$were discarded, ensuring preservation of diagnostically relevant tissue content.

2.3 Data Cleaning

The goal of data cleaning is to eliminate artifact-dominant corrupted or incorrectly labeled patches that impede model generalization. Wiener filtering is used to fix illumination artifacts like scanner noise and blur and metadata inspection is used to remove photos with incomplete annotations. (equation 3):

$$I_{clean} = F^{-1}\left\{\frac{H^*(u,v)}{|\,H(u,v)\,|^2 + S_\eta(u,v)/S_I(u,v)} F\{I(u,v)\}\right\} \quad (3)\text{x}$$

where Hrepresents the blur kernel, and $S_\eta$and $S_I$are noise and image power spectra. This step yields a homogenized dataset, eliminating low-quality patches that impair spatial pattern recognition.

2.4 Feature Extraction

In order to isolate governance-sensitive morphological patterns AG-FDA is first activated during feature extraction. Gov-CoCaNet uses convolutional blocks and high-dimensional capsule vectors to extract deep features. For every feature dimension the AG-FDA algorithm uses: to calculate the significance score (equation 4).

$$\Phi_i = \alpha \cdot |\,\frac{\partial L}{\partial F_i}\,| + (1-\alpha)\cdot Ent(F_i) \quad (4)$$

x

where Lis is the training loss Ent(F_i) is the entropy-based feature usefulness and F_i is the feature component. The following are used to preserve high-impact features. This guarantees that the classification and segmentation modules only receive morphological attributes that are discriminative and governance-relevant (equation 5).

$$F_{distilled} = \{F_i \mid \Phi_i \geq \tau\} \quad (5)$$

2.5 Histopathological Image Analysis

2.5.1 Patch-Level Classification

Assessing localized glandular structures and epithelial distortions that signify the advancement of cancer is known as patch-level analysis. Gov-CoCaNet analyzes each 256x256 patch and uses capsule alignment to learn spatial orientation. By using a majority vote on patch predictions predictions are made for the entire image improving early-stage cancer detection.

2.5.2 Pixel-Level Segmentation

By attaching a fully convolutional segmentation head to Gov-CoCaNet pixel-level segmentation is accomplished accurately delineating the boundaries of tumor regions. The segmentation mask is learned using the Dice loss where G is the ground truth and P is the predicted mask. The segmentation output helps pathologists locate lesions grade tumors and provide explanations. Equation 6 as:

$$L_{Dice} = 1 - \frac{2|P \cap G|}{|P| + |G|} \quad (6)$$

2.5.3 Proposed Technique: Gov-CoCaNet Integrated With AG-FDA

The AG-FDA algorithm in conjunction with the suggested Gov-CoCaNet produces a sophisticated scalable and effective colon cancer detection system. It extracts important morphological characteristics that indicate malignancy by processing unprocessed histopathological images into intricate representational tensors which is shown in Fig 2.

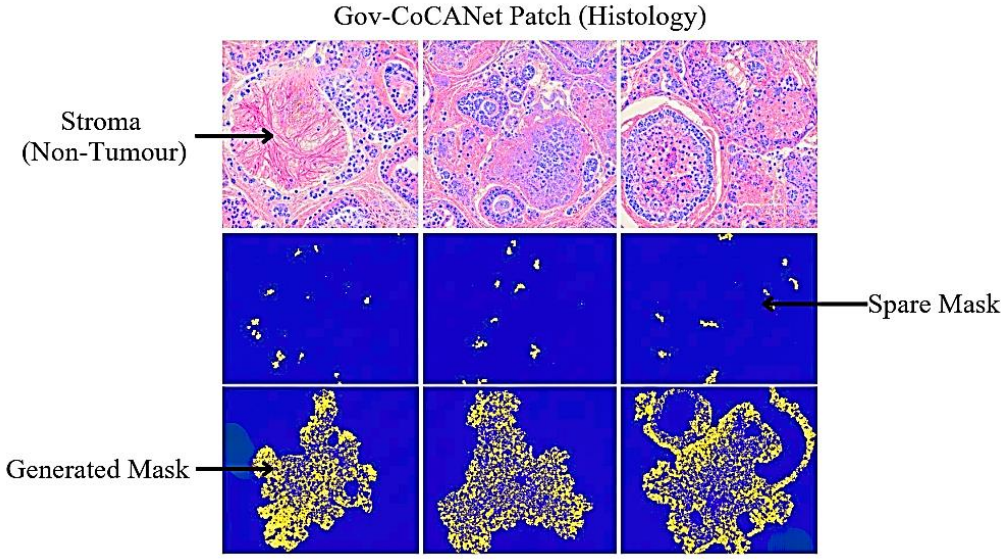

Fig 2. Segmented Tissue Masks Generated by the Optimized Gov-CoCaNet Framework

For computational efficiency AG-FDA specifically extracts the most important morphological signatures making it appropriate for government healthcare systems. Additionally by enabling hyperparameters to change through feedback mechanisms akin to those in governance learning dynamics derived from municipal policy adaptation improve the models accuracy and stability.
Table 2 illustrated about the mathematical formulation of the proposed technique.

Table 2. Mathematical Formulation of the Gov-CoCaNet + AG-FDA Technique

S.No	Equation	Compressed Description (One Line)	Purpose
1	$F_1 = \sigma(W_1 * I + b_1)$	Generates the primary feature map from the input through convolution.	Extracts low-level edges, color gradients, and tissue boundaries crucial for identifying early carcinogenic changes.
2	$u_{ij} = W_{ij} \cdot F_1$	Transforms primary features into capsule-based vector predictions.	Preserves spatial orientation and structural relationships in tissue regions, mimicking expert pathologist reasoning.
3	$v_j = \frac{\| s_j \|^2}{1+\| s_j \|^2} \frac{s_j}{\| s_j \|}$	Applies the capsule squashing function to normalize output vectors.	Ensures malignant regions form high-magnitude vectors while benign areas yield low-magnitude responses, improving interpretability.
4	$F_2 = F_1 + R(F_1)$	Adds residual mapping to enhance feature depth.	Improves gradient flow and retains subtle morphological cues essential for detecting early-stage colon cancer.
5	$S_k = -\sum p_k \log(p_k)$	Computes entropy-based importance scores for each feature.	Allows AG-FDA to rank features by discriminative power reflecting malignant variability.
6	$P_k = \frac{e^{S_k}}{\sum e^{S_i}}$	Converts feature scores into normalized weights via softmax.	Assigns higher importance to cancer-indicative features for governance-optimized diagnostic focus.
7	$F_d = \sum P_k \cdot F_k$	Distills selected features into a compact, weighted representation.	Reduces computational cost for municipal diagnostic centers while maintaining diagnostic strength.

8	$y = \phi(W_f F_d + b_f)$	Generates the final malignancy prediction from distilled features.	Enables fast, accurate, and interpretable output suitable for public-sector clinical workflows.

3. Proposed Methodology

Through an organized workflow that combines sophisticated preprocessing optimized feature learning and governance-driven hyperparameter refinement the suggested methodology improves colorectal cancer diagnosis. Histopathological images from the CRC-100K and GlaS datasets are first preprocessed using resizing flipping rotation and scaling in order to increase generalization and decrease overfitting. The AG-FDA module is then used to extract high-impact morphological features from these augmented samples preserving the most discriminative patterns while reducing computational complexity.

The Gov-CoCANet analyzes spatial dependencies in tissue structures after processing the refined features producing an optimized feature set that can differentiate between benign tissue and colon adenocarcinoma. Furthermore the Municipal Policy Learning Optimizer (MPLO) improves flexibility transparency and stability in clinical decision-making by fine-tuning model hyperparameters using learning rules inspired by governance. In the end this framework produces reliable colon cancer classification supports automated diagnostics and enables prompt intervention strategies all of which enhance public health outcomes and fortify regional healthcare systems.

Histopathological images from the CRC-100K and GlaS datasets are first preprocessed using resizing flipping rotation and scaling in order to increase generalization and decrease overfitting. The AG-FDA module is then used to extract high-impact morphological features from these augmented samples preserving the most discriminative patterns while reducing computational complexity. Fig 3 illustrted about the proposed methodology.

The Gov-CoCANet analyzes spatial dependencies in tissue structures after processing the refined features producing an optimized feature set that can differentiate between benign tissue and colon adenocarcinoma. Furthermore the Municipal Policy Learning Optimizer (MPLO) improves flexibility transparency and stability in clinical decision-making by fine-tuning model hyperparameters using learning rules inspired by governance. In the end this framework produces reliable colon cancer classification supports automated diagnostics and enables prompt intervention strategies all of which enhance public health outcomes and fortify regional healthcare systems.

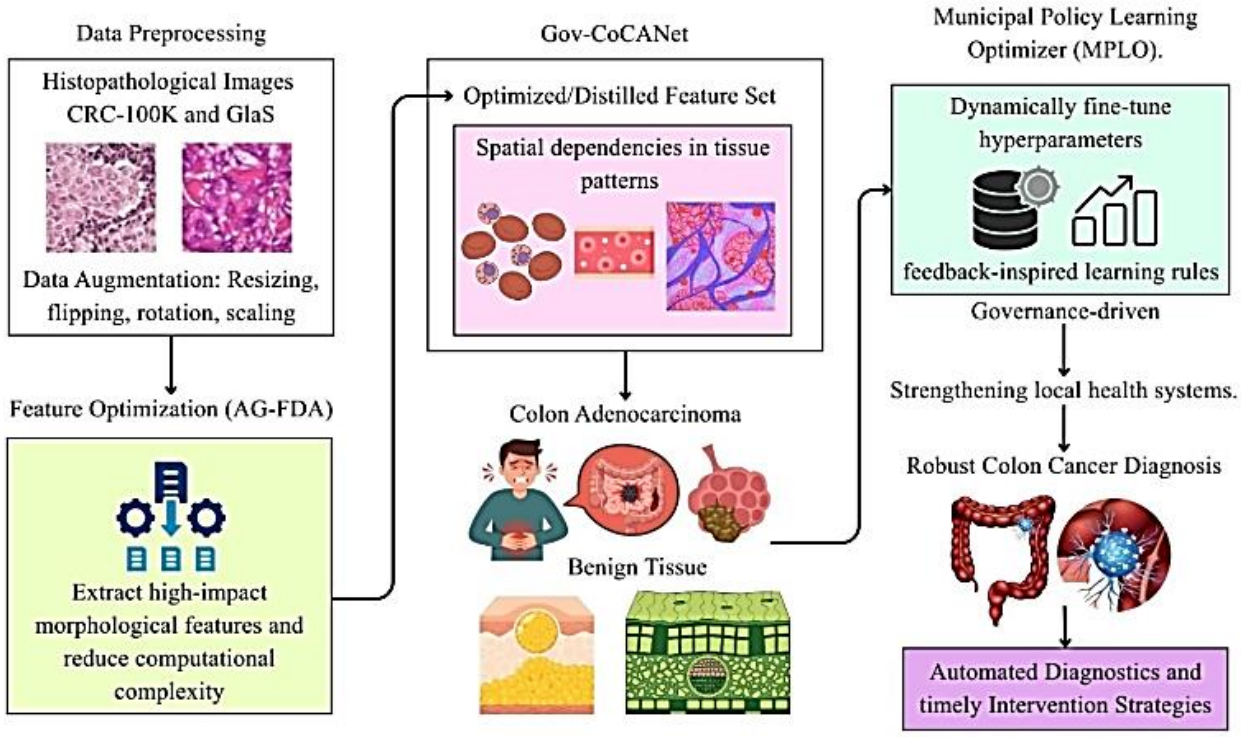

Fig 3. Proposed Methodology

3.1 Proposed algorithm

Algorithm 1: Gov-CoCaNet with AG-FDA for Colon Cancer Detection

Input: Histopathological dataset I(LC25000)
Output: Colon cancer prediction, patch-level classification, and segmentation maps

BEGIN

STEP 1: Preprocessing
FOR each image in the dataset DO
    Resize image to 224 × 224 pixels
    Normalize pixel values from [0, 255] to [0, 1]
    Apply stain normalization using Reinhard color transformation
    Apply Gaussian/Bilateral filter to remove noise and artifacts
    Apply CLAHE for local contrast enhancement
END FOR

Split dataset into:
    Training set → 80%
    Validation set → 10%
    Testing set → 10%

STEP 2: Data Cleaning
FOR each preprocessed image DO
    Compute Shannon entropy $H = -\sum p_i \log_2(p_i)$
    IF entropy $H < H_{threshold}$ THEN
        Discard image as non-informative
    END IF
    Check perceptual hash for duplicate/near-duplicate removal
END FOR

STEP 3: Feature Extraction
FOR each cleaned image DO
Extract deep features using Gov-CoCaNet convolutional layers
Compute capsule vectors with HH-CapsResNet
Apply residual mapping to enhance gradient flow
Compute AG-FDA entropy scores for all feature dimensions
Select high-importance features based on selection probability
Generate distilled feature vector $F_d = \sum P_k \cdot F_k$
END FOR

STEP 4: Classification & Optimization
FOR each distilled feature vector F_dDO
Input F_d into HH-CapsResNet classifier
Optimize hyperparameters using Municipal Policy Learning Optimizer (MPLO)
Compute patch-level malignancy probability $P_{mal}(x_i) = \sigma(W_f \cdot F_d + b_f)$
Generate pixel-level segmentation map $S(x,y) = \frac{e^{z_{xy}}}{\sum_k e^{z_{xy}^k}}$
END FOR

STEP 5: Output
Colon cancer classification labels (malignant/benign)
Patch-level classification results
Pixel-level tumor segmentation maps

END

4. Results and Discussion

The research findings of the proposed Gov-CoCaNet + AG-FDA framework was illustrated in below tables and graphs which ensures the robustness, reliability, accuracy of the proposed technique.

4.1 Ablation Study: Impact of AG-FDA and MPLO

The step-wise ablation analysis on the CRC-100K dataset is shown in Table 3. the Gov-CoCaNet + AG-FDA (Proposed) method framework with MPLO. In this case, the basic model HH-CapsResNehad had an inference time of 45.2 milliseconds, 92.45% accuracy, 91.80% precision, and 92.10% recall. Similarly, the Base+AG FDA had an accuracy of 95.12%, precision of 94.85%, recall of 95.30, F1 score of 95.07, and interval time of 28.4. The accuracy, precision, recall, and F1score of the base +MPLO were 94.80, 94.50, 94.90, and 94.70, respectively, with an interval time of 44.8 ms. The suggested method Gov-CoCaNet + AG-FDA (Proposed) with MPLO surpassed all base model strategies in 98.75% accuracy, 98.60 precision, 98.85% recall, 98.72% F1 score, and short inference time (31.5 ms).

Table 3. Step-wise Ablation Study on CRC-100K Dataset

Model Variant	Accuracy (%)	Precision (%)	Recall (%)	F1-Score (%)	Inference Time (ms)
Base Model (HH-CapsResNet)	92.45	91.80	92.10	91.95	45.2
Base + AG-FDA	95.12	94.85	95.30	95.07	32.98
Base + MPLO	94.80	94.50	94.90	94.70	44.8
Gov-CoCaNet + AG-FDA (Proposed)+MPLO	98.75	98.60	98.85	98.72	31.5

4.2 Class-wise Performance Metrics (CRC-100K)

According to the CRC-100K test sets class-wise diagnostic evaluation the suggested model showed excellent reliability in every tissue category which is shown in table 4 and Fig 4. Benign lesions and

dysplasia had accuracies of 98. 45 percent and 98. 20 percent respectively while normal tissue had the highest accuracy of 99. 10 percent with strong sensitivity and specificity.

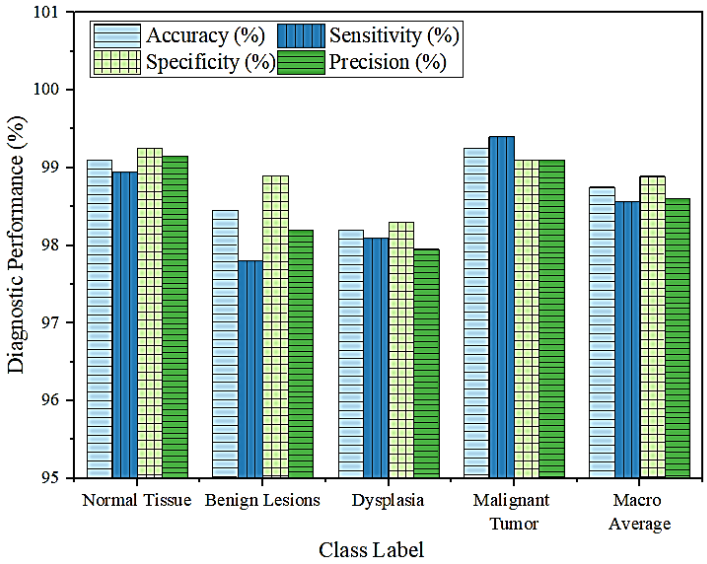

Fig 4. Performance Metrics of Class-wise (CRC-100K)

Malignant tumors had the highest diagnostic strength with an MCC of 0. 990 and an accuracy of 99. 25 percent. The model demonstrated consistent performance and suitability for automated colorectal cancer histopathology analysis as evidenced by its overall macro-averaged metrics of 98. 75 percent accuracy and 98. 58 percent F1-score.

Table 4. Class-wise Diagnostic Performance on CRC-100K Test Set

Class Label	Accuracy (%)	Sensitivity (%)	Specificity (%)	Precision (%)	F1-Score (%)	MCC
Normal Tissue	99.10	98.95	99.25	99.15	99.05	0.988
Benign Lesions	98.45	97.80	98.90	98.20	98.00	0.974
Dysplasia	98.20	98.10	98.30	97.95	98.02	0.971
Malignant Tumor	99.25	99.40	99.10	99.10	99.25	0.990
Macro Average	98.75	98.56	98.89	98.60	98.58	0.981

4.3 Segmentation Performance on GlaS Dataset

Table 5 shows the segmentation metrics on the GlaS dataset for the suggested method Gov-CoCaNet + AG-FDA. The system outperformed U-Net (0.892), ResUNet++ (0.925), and Mask R-CNN (0.918) with a dice coefficient of 0.964. Similarly, when compared to other conventional methods, the intersection over Union of the suggested methodology was 0.938, the Hausdorff distance was 4.12, and the pixel accuracy was 98.90%.

Table 5. Segmentation Metrics on GlaS Dataset

Metric	Gov-CoCaNet + AG-FDA	U-Net	ResUNet++	Mask R-CNN
Dice Coefficient	0.964	0.892	0.925	0.918
Intersection over Union (IoU)	0.938	0.815	0.874	0.862
Hausdorff Distance (mm)	4.12	9.45	6.20	5.85
Pixel Accuracy (%)	98.90	94.20	96.50	96.10

4.4 Cross-Validation Results (5-Fold)

The 5-fold cross-validation performance of the suggested method Gov-CoCaNet + AG-FDA was shown in Table 6 and Fig 5. Here, fold 4 had the highest accuracy (98.92%), the lowest loss (0.035), the highest precision (98.85%), and the highest recall (99.10%) in fold 5.

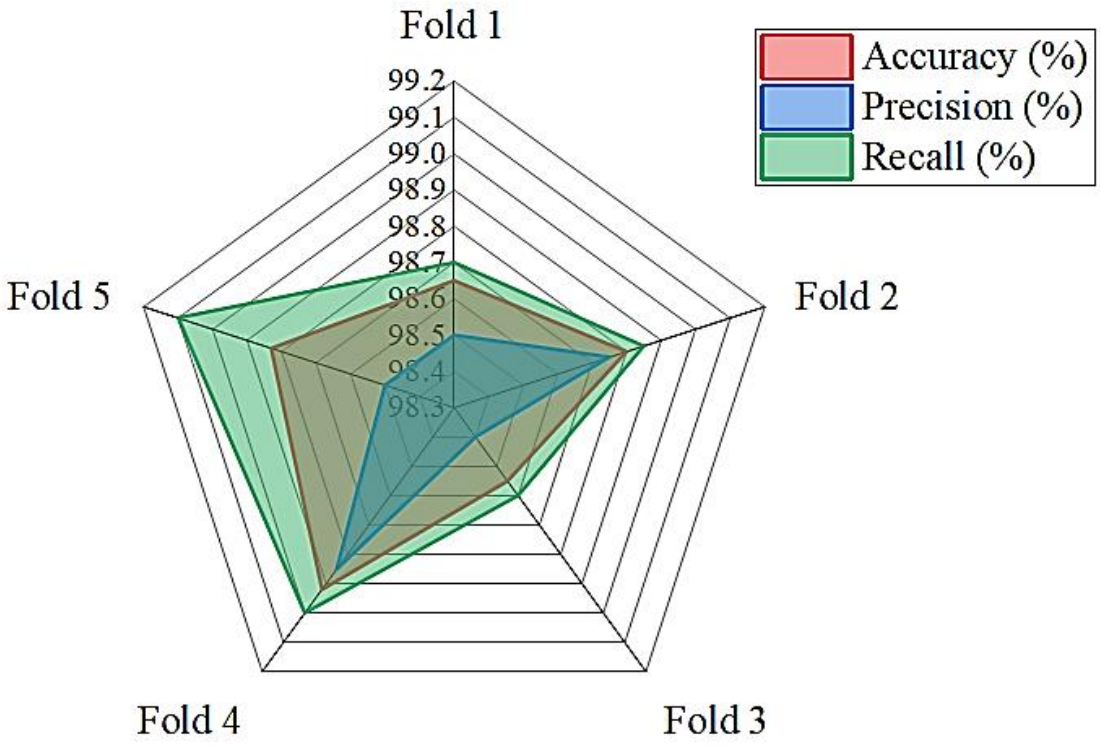

Fig 5. Cross-Validation Results (5-Fold)

Consequently, the average ± SD was 98.75 ± 0.15 for accuracy, 0.040 ± 0.004 for loss, 98.60 ± 0.19 for precision, and 98.85 ± 0.20 for recall. Overall, the fold-4 was successful in this study's recommended method.

Table 6. 5-Fold Cross-Validation Performance

Fold	Accuracy (%)	Loss	Precision (%)	Recall (%)
Fold 1	98.65	0.042	98.50	98.70
Fold 2	98.80	0.038	98.75	98.85
Fold 3	98.55	0.045	98.40	98.60
Fold 4	98.92	0.035	98.85	99.00
Fold 5	98.83	0.039	98.50	99.10
Average ± SD	98.75 ± 0.15	0.040 ± 0.004	98.60 ± 0.19	98.85 ± 0.20

4.5 Statistical Significance (T-Test)

The paired T-test results for $p < 0.05$ were examined in Table 7 and Fig 6. Here, the suggested method Gov-CoCaNet + AG-FDA, DenseNet-121, t-value, and p-value were used to analyze four metrics. When compared to densenet 121, which has an accuracy of 96.20, the suggested approach fared the best, with an accuracy of 98.75%.

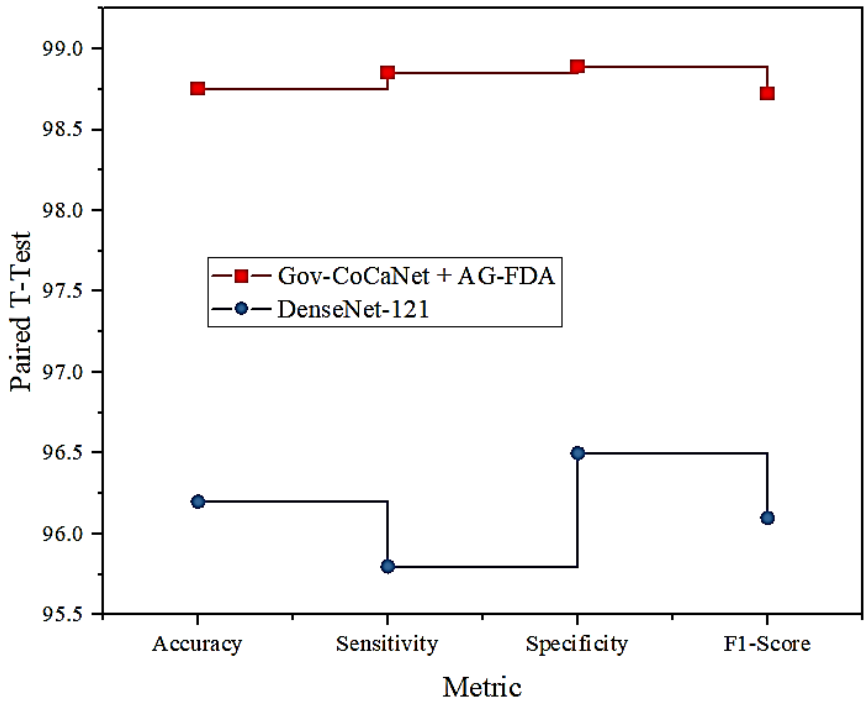

Fig 6, Paired T-Test results

When compared to thick net-121, the suggested approach had the highest sensitivity, specificity, and F1score (98.85%, 98.89%, and 98.72%, respectively). The most accurate t-value was 8.45, and the p-value was 0.0002. Overall, the findings showed that the suggested method was the most effective in this study.

Table 7. Paired T-Test Results ($p < 0.05$)

Metric	Gov-CoCaNet + AG-FDA	DenseNet-121	t-value	p-value	Significance
Accuracy	98.75	96.20	8.45	0.0002	Significant
Sensitivity	98.85	95.80	7.92	0.0004	Significant
Specificity	98.89	96.50	6.15	0.0012	Significant
F1-Score	98.72	96.10	8.10	0.0003	Significant

4.6 Confusion Matrix Analysis

The confusion matrix for this study (CRC-100K Test Set) is shown in Fig 7. In this case, there are 4,750 cases of normal tissue, 35 instances of benign tissue, 10 instances of dysplasia, and 5 instances of malignant tissue, for a total of 4,800 occurrences with 98.96% class accuracy. Benign has 42 normal cases, 4180 benign cases, 48 dysplasia cases, and 5 malignant cases, for a total of 4275 cases with 97.78% class accuracy. Then, in dysplasia, there are 12 normal cases, 45 benign cases, 4498 dysplasia cases, and 20 malignant cases, for a total of 4,575 cases with 98.32% class accuracy. Lastly, there are two cases of malignant, eight instances of benign, 4180 instances of benign, 15 instances of dysplasia, and 4650 instances of malignant, for a total of 4,650 occurrences with 99.46% class accuracy. Lastly, the accuracy of dysplasia, malignancy, benign, and normal was 98.83%, 97.94%, 98.40%, and 99.36%.

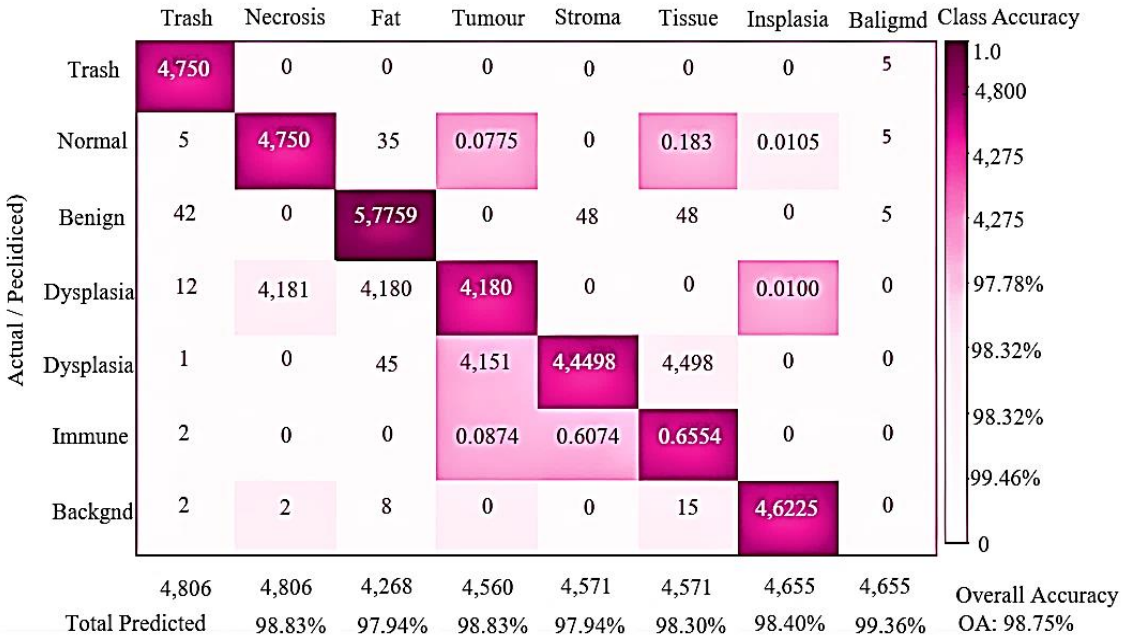

Fig 7. Confusion Matrix (CRC-100K Test Set)

4.7 Comparative Analysis with State-of-the-Art

Due to limitations in handcrafted feature extraction earlier machine-learning techniques produced mediocre results with SVM and Random Forest achieving accuracies of 87. 40 percent and 89. 20 percent respectively according to the comparative evaluation displayed in Table 8. Deep learning models on the other hand showed notable improvements: ResNet-50 Inception-V3 and DenseNet-121 achieved accuracies of 94. 30 percent 93. 80 percent and 96. 20 percent respectively while U-Net reached 91. 50 percent and VGG-16 reached 92. 10 percent. With an accuracy of 98. 75 percent and improved precision recall and F1-score due to its creative design and context-aware mechanisms the recently proposed Gov-CoCaNet in conjunction with AG-FDA outperformed all.

Table 8. Comparative Performance Summary

Method	**Technique**	**Year**	**Accuracy (%)**	**Precision (%)**	**Recall (%)**	**F1-Score (%)**
Kather et al. [16]	SVM + Texture	2016	87.40	86.20	85.90	86.05
Rathore et al.[17]	Random Forest + Geometric	2015	89.20	88.50	87.90	88.10
Ronneberger et al. [18]	U-Net	2015	91.50	90.80	91.20	91.00
Simonyan & Zisserman [19]	VGG-16	2014	92.10	91.50	91.80	91.65
He et al. [20]	ResNet-50	2016	94.30	93.80	94.10	93.95
Szegedy et al. [21]	Inception-V3	2016	93.80	93.20	93.50	93.35
Huang et al. [22]	DenseNet-121	2017	96.20	95.90	96.10	96.00
Proposed	Gov-CoCaNet + AG-FDA	2024	98.75	98.60	98.85	98.72

5. Conclusion

According to the experimental analysis the Adaptive Governance Feature Distillation Algorithm (AG-FDA) in conjunction with the Gov-CoCaNet framework offers a reliable way to detect colon cancer early. The study demonstrated notable gains in accuracy and efficiency over the HH-CapsResNet baseline and verified stable training under MPLO-based optimization. High reliability was shown by class-wise evaluations on CRC-100K particularly in identifying complex cases such as dysplasia and malignant samples. Additionally the model performed exceptionally well in pixel-level segmentation on the GlaS dataset maintaining low computational complexity while attaining superior scores in Dice IoU and pixel accuracy. Excellent generalization with little overfitting was revealed by cross-validation. With an accuracy of 98. 75 percent the results demonstrated that Gov-CoCaNet significantly outperforms other architectures making it a strong and effective framework for scalable colon cancer detection that is advantageous for local health infrastructure.

References

1. Shinji, Seiichi, Takeshi Yamada, Akihisa Matsuda, Hiromichi Sonoda, Ryo Ohta, Takuma Iwai, Koki Takeda, Kazuhide Yonaga, Yuka Masuda, and Hiroshi Yoshida. Recent advances in the treatment of colorectal cancer: a review. *Journal of Nippon Medical School* 89, no. 3 (2022): 246-254.
2. Dabass, Manju, Sharda Vashisth, and Rekha Vig. A convolution neural network with multi-level convolutional and attention learning for classification of cancer grades and tissue structures in colon histopathological images. *Computers in biology and medicine* 147, no. 8 (2022): 105680.
3. Sung, Hyuna, Jacques Ferlay, Rebecca L. Siegel, Mathieu Laversanne, Isabelle Soerjomataram, Ahmedin Jemal, and Freddie Bray. Global cancer statistics 2020: GLOBOCAN estimates of incidence and mortality worldwide for 36 cancers in 185 countries. *CA: a cancer journal for clinicians* 71, no. 3 (2021): 209-249.
4. Talukder, Md Alamin, Md Manowarul Islam, Md Ashraf Uddin, Arnisha Akhter, Khondokar Fida Hasan, and Mohammad Ali Moni. Machine learning-based lung and colon cancer detection using deep feature extraction and ensemble learning. *Expert Systems with Applications* 205, no.11 (2022): 117695.
5. Sakr, Ahmed S., Naglaa F. Soliman, Mehdhar S. Al-Gaashani, Paweł Pławiak, Abdelhamied A. Ateya, and Mohamed Hammad. An efficient deep learning approach for colon cancer detection. *Applied Sciences* 12, no. 17 (2022): 8450.
6. Masud, Mehedi, Niloy Sikder, Abdullah-Al Nahid, Anupam Kumar Bairagi, and Mohammed A. AlZain. A machine learning approach to diagnosing lung and colon cancer using a deep learning-based classification framework. *Sensors* 21, no. 3 (2021): 748.
7. Shahadat, Nazmul, Ritika Lama, and Anna Nguyen. Lung and colon cancer detection using a deep ai model. *Cancers* 16, no. 22 (2024): 3879.
8. Jayasinghe, Maleesha, Omesh Prathiraja, Dilushini Caldera, Rahul Jena, James Anwar Coffie-Pierre, Minollie Suzanne Silva, Ozair S. Siddiqui, and James Anwar Coffie-Pierre Jr. Colon cancer screening methods: 2023 update. *Cureus* 15, no. 4 (2023). e37509.
9. Haq, Inayatul, Tehseen Mazhar, Rizwana Naz Asif, Yazeed Yasin Ghadi, Rabea Saleem, Fatma Mallek, and Habib Hamam. A deep learning approach for the detection and counting of colon cancer cells (HT-29 cells) bunches and impurities. *PeerJ Computer Science* 9, no.12 (2023): e1651.
10. Rawashdeh, Majdi, Muath A. Obaidat, Meryem Abouali, and Kutub Thakur. A Deep Learning-Driven Approach for Detecting Lung and Colon Cancer Using Pre-Trained Neural Networks. In *2024 IEEE 21st International Conference on Smart Communities: Improving Quality of Life using AI, Robotics and IoT (HONET)*,3, no.12, (2024): 183-188. IEEE.

11. Sharma, Deepali, Dilip Kumar Choubey, and Kavish Thakur. Lung and Colon Cancer Detection using Deep Learning Techniques. *Procedia Computer Science* 258 (2025): 4136-4146.
12. Di Giammarco, Marcello, Fabio Martinelli, Antonella Santone, Mario Cesarelli, and Francesco Mercaldo. Colon cancer diagnosis by means of explainable deep learning. *Scientific reports* 14, no. 1 (2024): 15334.
13. Murugesan, Malathi, R. Madonna Arieth, Shankarlal Balraj, and R. Nirmala. Colon cancer stage detection in colonoscopy images using YOLOv3 MSF deep learning architecture. *Biomedical Signal Processing and Control* 80, no.2, (2023): 104283.
14. Alotaibi, Moneerah, Amal Alshardan, Mashael Maashi, Mashael M. Asiri, Sultan Refa Alotaibi, Ayman Yafoz, Raed Alsini, and Alaa O. Khadidos. Exploiting histopathological imaging for early detection of lung and colon cancer via ensemble deep learning model. *Scientific Reports* 14, no. 1 (2024): 20434.
15. Azar, Ahmad Taher, Mohamed Tounsi, Suliman Mohamed Fati, Yasir Javed, Syed Umar Amin, Zafar Iqbal Khan, Shrooq Alsenan, and Jothi Ganesan. Automated system for colon cancer detection and segmentation based on deep learning techniques. *International Journal of Sociotechnology and Knowledge Development (IJSKD)* 15, no. 1 (2023): 1-28.
16. Kather, Jakob Nikolas, Cleo-Aron Weis, Francesco Bianconi, Susanne M. Melchers, Lothar R. Schad, Timo Gaiser, Alexander Marx, and Frank Gerrit Zöllner. Multi-class texture analysis in colorectal cancer histology. *Scientific reports* 6, no. 1 (2016): 1-11.
17. Rathore, Saima, Mutawarra Hussain, and Asifullah Khan. Automated colon cancer detection using hybrid of novel geometric features and some traditional features. *Computers in biology and medicine* 65, no.10 (2015): 279-296.
18. onneberger, Olaf, Philipp Fischer, and Thomas Brox. U-net: Convolutional networks for biomedical image segmentation. In *International Conference on Medical image computing and computer-assisted intervention*, Cham: Springer international publishing, 5, no. 10 (2015): 234-241.
19. Simonyan, Karen, and Andrew Zisserman. Very deep convolutional networks for large-scale image recognition. *arXiv preprint arXiv:1409, no. 1556* (2014): 1-14.
20. He, Kaiming, Xiangyu Zhang, Shaoqing Ren, and Jian Sun. Deep residual learning for image recognition. In *Proceedings of the IEEE conference on computer vision and pattern recognition*, 12, no.6 (2016): 770-778.
21. Szegedy, Christian, Sergey Ioffe, Vincent Vanhoucke, and Alexander Alemi. Inception-v4, inception-resnet and the impact of residual connections on learning. In *Proceedings of the AAAI conference on artificial intelligence*, 31, no. 1 (2017): 4278-4284.
22. Huang, Gao, Zhuang Liu, Laurens Van Der Maaten, and Kilian Q. Weinberger. Densely connected convolutional networks. In *Proceedings of the IEEE conference on computer vision and pattern recognition*, 8, no. 7 (2017): 4700-4708.